IDENTIFICATION OF PARALLEL HETEROGENEITIES WITH MISCIBLE DISPLACEMENT

C.Dauba[1,2], G.Hamon[1], M.Quintard[3], F.Cherblanc[2].
[1] Elf Exploration Production, Pau, France.
[2] L.E.P.T.ENSAM (UA CNRS), Bordeaux, France.
[3] Institut de Mécanique des Fluides de Toulouse, Toulouse, France.

The identification of heterogeneity parallel to layers is commonly considered as a very important parameter in the dynamic characterization of core samples. However, such a characterization often appears to be extremely difficult to realize.
To determine the existence of longitudinal heterogeneity such as preferential paths, fractures or double porosity porous media, we performed miscible displacement on samples before waterflood experiments. Miscible displacement is very simple to perform and it allowed us to reject the most heterogeneous samples. We present experimental work of miscible displacement realized on seven samples. Miscible experiments have been performed at different Peclet numbers. In addition, we present unsteady-state relative permeability curves for the eight samples. We have also computed 2D finely gridded simulations of miscible flow through heterogeneous cores. These simulations perfectly illustrate relative impact of heterogeneity geometry on effluent concentration data.
Conclusions of this work are :
1°) samples which present typical longitudinal heterogeneity through miscible displacement result in strongly anomalous relative permeability curves. 2°) On the other hand, if miscible displacement reveals sample curves close to homogeneous ones, the samples concerned present homogeneous relative permeability curves. 3°) For all the cases presented, the heterogeneity spatial organization deduced from 2D simulations is in very good agreement with indications of heterogeneity geometry coming from other sources (2D surface maps of probe permeameter measurements, CT scan data...).
4°) It confirms that miscible displacement is a very simple method for dynamic identification of the most heterogeneous samples. To perform miscible displacement can avoid long and expensive coreflooding tests, inevitably doomed to failure because of strong longitudinal heterogeneity.

Introduction

Water/oil relative permeability curves are usually obtained on carefully selected, homogeneous core samples. This assumption might be violated if samples contain lengthwise heterogeneity such as fractures, high permeability thin streaks or connected vugs. As unsteady state coreflood is very sensitive to the longitudinal heterogeneity, the interpretation of water/oil production curves with a 1D numerical model or standard JBN may lead to anomalous relative permeabilities. It means that performing coreflood experiments on well selected homogeneous samples is particularly important to avoid expensive but useless experiments.
However, for some samples, relative permeability curves are absolutely necessary even if the core samples present strong heterogeneity and if the homogeneity assumption is not longer valid. In these cases, a correct interpretation requires the use of a 2D or 3D heterogeneous representation of the core sample. Obtaining a detailed representation is difficult, and may not be practical on a industrial basis. However, the overall behavior of the core sample may be characterized by simple classes of heterogeneous materials with parameters such as the permeability contrast and the volume proportion of different heterogeneous zones. The present paper demonstrates that such an identification of the lengthwise heterogeneity can be easily made by the interpretation of miscible displacement.
One of the objectives of the present paper is to confirm that performing miscible experiment could represent a simple method for rejecting the most heterogeneous samples before the reservoir conditions relative permeability measurements. Several types of measurements are routinely performed to select the most homogeneous but representative samples used for core flooding test : closely spaced minipermeameter measurements (Dauba, 1998), 3D computed tomography (CT) density, 1D X-Ray or Gamma-Ray profiles. Advantages and drawbacks of these methods are briefly reviewed by a companion paper SCA 9949. It is our

experience that detection of slightly deconsolidated zones on unconsolidated reservoir samples or samples spanning paths of connected vugs is rather subjective with CT scan. Moreover, on vuggy cores, CT delivers a porosity map which can hardly be correlated with permeability (Dauba, 1998).
A preliminary study has already been carried out to define the relation between miscible and unsteady-state two-phase displacements. Figures 1 and 2 illustrate the empiric relation between relative permeability curves and the miscible displacement curve : both are very sensitive to lengthwise heterogeneity. Sample X1, which has anomalous relative permeability curves, also features a miscible curve with an early breakthrough and a long tail. On the contrary, the sample X2 has homogeneous responses for both miscible and two-phase displacements. This empirical observation confirms us that miscible displacement allows the detection of heterogeneous core samples susceptible of providing anomalous relative permeability curves.

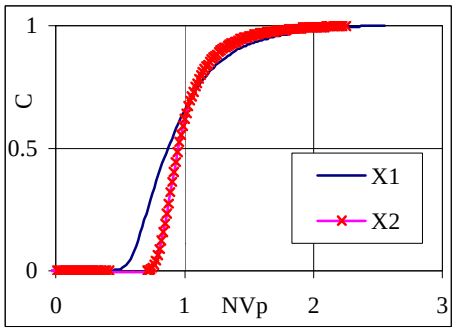

Figure 1 - Miscible Curves of the samples X1 and X2

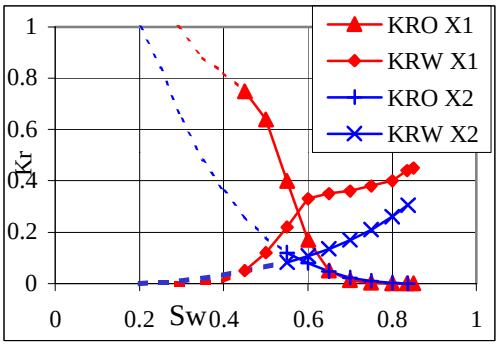

Figure 2 - Unsteady-state water/oil relative permeability curves of the samples X1 and X2.

Most of the studies devoted to the interpretation of miscible displacement in heterogeneous porous media are based on models containing an immobile fluid phase [Coats & Smith, 1964 ; Mennela & al., 1997 ; Baker, 1975]. Only a few consider that tracer may be mobile in the whole pore system [Gerke & van Genuchten, 1993 ; Quintard & al., 1998]. These latter models are more general since they also include the mobile/immobile zone behavior. Therefore, our model involves two zones at the macroscopic level -a high permeable region and a less permeable matrix system- and the miscible fluids in both systems are assumed to be mobile. Finely gridded 2D simulations of miscible displacement were carried out for typical cases of heterogeneity. Based on this knowledge, we present the identification from miscible displacement curves of lengthwise heterogeneity structures in terms of geometry, permeability contrast and flow rate.
Then, this methodology is applied to the interpretation of real experiments. Miscible displacements of seven core samples are presented. In addition to the miscible curves, we show unsteady-state relative permeability curves. Thanks to type curves and heterogeneity geometry indications coming from CT scan and/or probe-permeameter, we succeeded in matching simulated miscible curves to the experimental ones. Simulation parameters allowed us to determine proportion of high and low permeable regions and permeability contrast.

Principle of experimental miscible displacement

Miscible displacement consists of the injection at constant rate of a tracer. It is important to note that core samples are set vertical during miscible experiments in order to avoid gravity effect across longitudinal layers.
Two salt-water solutions of different concentration [C] were used as a tracer. The two brines were mixtures of NaCl, KCl, $CaCl_2$ and $MgCl_2$ and they had respective concentrations of 30g/l and 120g/l of equivalent NaCl. Into a sample previously saturated in the 30 g/l brine, we started abruptly to inject the 120 g/l brine at a constant rate. The in-situ fluid was progressively displaced by the 120 g/l brine. The variation of the tracer concentration was determined at very short regular intervals through a density measurement at the outlet of the core. The curve obtained was a plot of the effluent concentration as a function of the injected pore volume (Vp). Tracer displacement is a low cost measurement which is also very easy to carry out. The

routine of miscible displacement is simple : measurements are automated and the data are written on a disk. Moreover, experiments are realized in ambiant conditions and the fluids used are brines.

Simulations of miscible displacement

The theoretical framework for our interpretation of the miscible experiments is based on the following ideas. While anomalous dispersion due to heterogeneities may require highly complex descriptions involving time and spatial convolutions, it has been shown in Quintard and Whitaker (1998) and Ahmadi et al. (1998) that two-equation models can represent a wide range of heterogeneity effects with a minimum of parameters. In these papers, a general two-equation model has been proposed that incorporate the effect of mobile/immobile zones, as well as more general systems with advection and diffusion/dispersion in both regions. The model involves several parameters such as the volume fraction of these zones, the large-scale transport properties, i.e., permeability and dispersion tensors for both regions in the two equation model, etc… The underlying heterogeneity in such systems may be very complex. However, a small number of systems featuring simple geometry can be proposed that will be representative of most of the two-equation behavior. Such heterogeneous systems correspond for example to cross-sectional barriers, or layered samples. The idea is to associate to a given experiment one of these representative heterogeneous systems. This representation will be used subsequently, for instance, to check through direct simulations whether anomalous relative permeability curves may be expected. Of course, in the absence of additional information, it is impossible to say that the real system corresponds exactly to the heterogeneity in the associated system. However, they are expected to have the same large-scale behavior, which is enough to interpret our laboratory-scale experiments in a very predictive manner.
Partial results for these elementary systems are presented below.

1- Simulation of miscible displacement for 1D homogeneous cores

The case of 2D miscible flow is very classical and the results are given without much detail. The convection-dispersion equation is used to compute the miscible response of an homogeneous, semi-finite and isotropic porous medium. We consider both hydrodynamic dispersion and molecular diffusion and the tracer is ideal. The tracer distribution is governed by [Bear, 1972] :

$$\frac{dC}{dt} + \frac{v}{e}\frac{dC}{dx} = \frac{\mathbf{D}}{e}\frac{d^2C}{dx^2} \qquad (1)$$

With normalized concentrations, initial and boundary conditions are :

$$C(x=0,t)=1$$
$$C(x,t=0)=0$$
$$\lim_{x\to\infty} C(x,t)=0 \qquad (2)$$

The analytical solution is written in a dimensionless form using the Peclet number ($\mathrm{Pe}=\frac{\mathrm{vL}}{\mathrm{D}}$), a dimensionless time ($\tau = vt/(\varepsilon L)$) and x= L :

$$C(L,t)=\frac{1}{2}erfc\left(\frac{1}{2}\frac{1-t}{\sqrt{\frac{t}{Pe}}}\right)+\frac{1}{2}\exp(Pe)erfc\left(\frac{1}{2}\frac{1+t}{\sqrt{\frac{t}{Pe}}}\right) \qquad (3)$$

For large Pe numbers (i.e. high velocity), the second term can be neglected. The effluent flowing concentration is calculated only from the first term of equation (3). By definition, the concentration measured at time associated with one injected pore volume (Vp), t=L/vε, will always be 0.5 for normalized concentrations, as shown on curve noticed $v=10^{-6}$ m/s of figure 3.

However, one must not forget that, for low Pe values (i.e. low velocity), the second term of equation (3) is not negligible compared with the first term. The effect of the second term is to shift the curve given by the first term of equation (3) upward ; this is well documented by Correa & al.(1990). Thus the effluent concentration measured at 1 Vp injected will always be larger than 50%. The shift introduced by the second

term at low velocity is illustrated in figure 3 by the curve v=10^{-8} m/s of figure 3. This figure illustrates also the influence of velocity on a homogeneous core sample : spreading increases with decreasing flow rate. Figure 4 reveals the impact of permeability (correlated to dispersivity) : a high permeable sample leads to a profile more spread around the x=1 Vp axis.

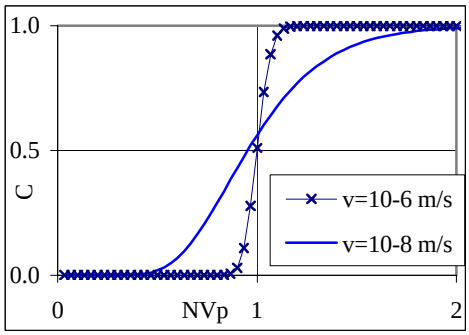

Figure 3 –Homogeneous 1D model : Influence of v, K= 5 mD.

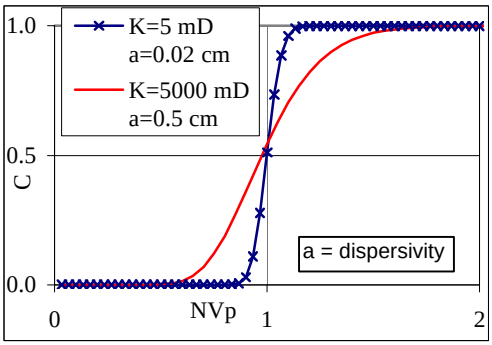

Figure 4 –Homogeneous 1D model : Influence of permeability and dispersivity, v= 10^{-6} m/s.

2- Simulations of miscible displacement for 2D heterogeneous cores.

- Two-dimensional numerical model

A numerical transport model, referred to as Transp, has been used to simulate the miscible displacement of a tracer in heterogeneous porous media considering advection and dispersion (including both mechanical dispersion and diffusion). Transp is integrated with Modflow, a 2D ground-water flow model that uses implicit finite-difference methods to solve the flow equation. Transp uses the method of characteristics to solve the transport equation on the basis of the hydraulic gradients computed with the flow model. The method of characteristics uses particle tracking to represent advective transport and a 9 points implicit finite-difference method to calculate the effects of hydrodynamic dispersion

After the normalization of the concentration field, the initial condition is written as :

$$C(x,y,t=0)=0 \qquad \text{on the simulated domain}$$

The boundary conditions associated with the tracer injection at constant rate in a porous medium are the following :

$$C(x=0,y,z,t)=1 \tag{4}$$

$$\left.\frac{dC}{dx}\right|_{x=L,t}=0 \tag{5}$$

About numerical dispersion, the method of characteristics used to solve the transport equation has a very small numerical dispersion.

- Typical responses according to heterogeneity geometry, velocity and permeability contrast

Miscible displacements were computed for many types of 2D heterogeneity geometry : cross-section heterogeneity and longitudinal heterogeneity. We assume the 2D simulated core sample consists of two different regions : a high permeable region and a low permeable zone. The 2D simulated core sample is divided into 100 cells for the 20 cm length and 25 cells for the 5 cm diameter. The input data of the simulator are geometry, permeability, porosity and dispersivity of each region, the total flow rate and the core length. A value of dispersivity (comprise between 0.2 mm and 5 mm) is associated with each permeability range. As output, the simulator provides the variation of the effluent concentration as a function of time. In this paper, it must be noticed that we always represent graphically the concentration variation as a function of the injected pore volume (Vp). Velocity, permeability contrast and geometry were varied in order to obtain type curves. Only a few examples are presented in this paper.

- Cross-section heterogeneity

Figure 5 presents the miscible response of a cross-section heterogeneity illustrated by figure 6. Curves of homogeneous cores are associated. We note that there is no significant difference between the cross-section

heterogeneity curve and the homogeneous ones, even if the permeability contrast of the cross-section case is about 100 and high permeable region volume proportion is 30%. It seems that miscible displacement is not very sensitive to the cross-section heterogeneity. Other methods should be used to detect series heterogeneity, for instance probe permeameter measurements when possible, or X ray or Gamma ray profiles.

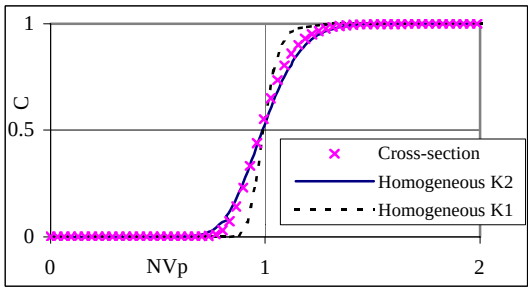

Figure 5 –Cross-section heterogeneity : phi2= 30%, K1=5 mD, K2=500 mD; v= 10^{-6} m/s.

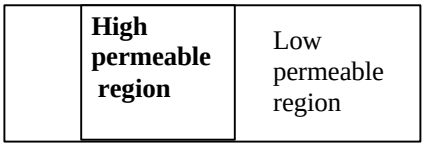

Figure 6 –Geometry of cross-section heterogeneity.

- Case 40

Figures 8, 9 and 11 correspond to lengthwise heterogeneity type, referred as Case 40 and illustrated by figure 7. For Case 40, an along-axis sample spanning high permeability region is embodied in a low permeability region. Figure 8 illustrates the influence of velocity on Case 40. At the highest rate v=10^{-6} m/s, we observe a sharp curve and a break at x=0.8 Vp followed by a tail. This behaviour is typical of a mobile/immobile system. At lowest injection rates, the effluent curve trends to "homogeneous" response. It seems that miscible responses of the two regions are more differentiated at high flow rates. As a matter of fact, high velocity leads to less mass exchange between the two regions. Low velocity enables more diffusive process and, thus, more homogeneization between regions. It confirms that lengthwise heterogeneity identification is easier at high velocities [Correa & al., 1990].

The impact of volume proportion (related to the high permeable region thickness, cf. figure 7) is represented for Case 40 in figure 11 .The permeability contrast is about 100. When the high permeability region is very thin (only 12% of the total volume), the breakthrough is for 0.15 Vp. When the high permeability region is 40% of the volume, the breakthrough occured at x=0.4 Vp. As expected from the physics involved, we can conclude that the cumulative throughput at breakthrough is in close agreement with the volumetric fraction of high permeability region for the strong permeability contrast.

The effect of the variation of the contrast in permeability and dispersivity is illustrated in figure 9. As the contrast increases, the tail is more important; the curve is reaching the final concentration at 3.5 Vp for a permeability ratio of 10 instead of 5 Vp for a permeability ratio of 1000. In all our numerical simulations,we found that *a long tail is typical of a strong permeability contrast.*

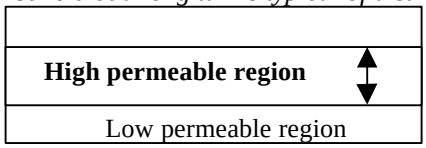

Figure 7 – Geometry of Case 40.

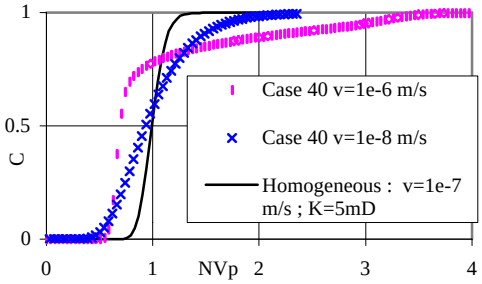

Figure 8 – Case 40 : phi2= 40%, K1= 5 mD ; K2= 50 mD, Influence of v.

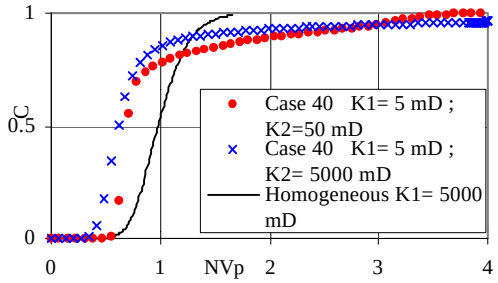

Figure 9 – Case 40 : phi2= 40%, v= 10^{-6} m/s. Influence of permeability contrast.

Low permeable region
High permeable region

Figure 10 – Geometry of Case 50

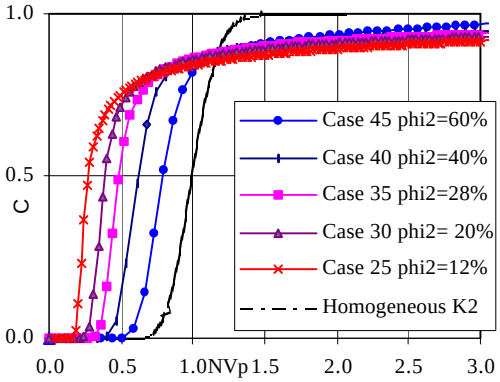

Figure 11 – Case 40 : K2=500 mD, K1=5 mD,v=10^{-6} m/s. Influence of the volume proportion.

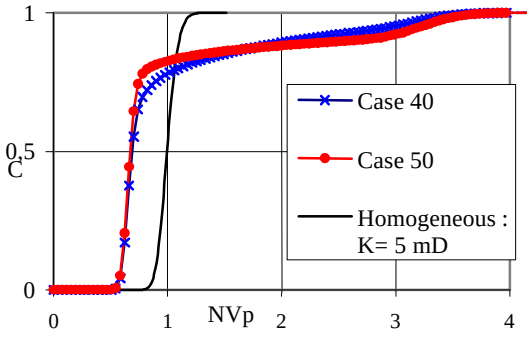

Figure 12 – Case 40 and Case 50 : phi2= 40%, K1 =5 mD, K2 =50 mD, v=10^{-6} m/s.

- Case 50

Case 50 is described on figure 10. A sample spanning high permeability region is located at the bottom of the core sample. For the same permeability contrast and the same volume proportion, the results for Case 40 and Case 50 present a few differences in figure 12. For Case 50, the miscible responses of the two regions are more differentiated than those of the Case 40. For Case 50, the high permeability region is at the bottom of the core, so there is less exchange surface between the two regions than for Case 40, and the characteristic length for diffusion accross the low permeable region is larger, thus leading to lower mass exchange coefficients (Ahmadi et al., 1998).

- Case 60

Case 60 is described in figure 13. A high permeable inclusion is embodied in a low permeable core. Figure 15 illustrates the influence of velocity for Case 60 with a 10 permeability ratio. The curve for Case 60 presents two steps at high velocity (v=10^{-5} m/s) and with a permeability ratio of 10. At low velocity, the gap between the regions diminishes a bit and the miscible response trends to the homogeneous one. Again high rate miscible tracer tests highlight heterogeneity. The impact of the permeability contrast is shown in figure 14. The miscible curve consists of two steps for a permeability contrast of 10. When the permeability contrast increases, the two-step curves are transformed into a long-tail curve for a contrast of 1000. Same behaviors were found with the two other geometries. In conclusion, a long-tail curve is typical of a very high permeability ratio, whereas *two distinct steps are significant of a less contrasted permeability ratio.*

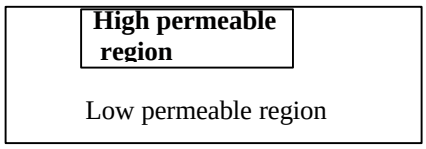

Figure 13 – Geometry of Case 60.

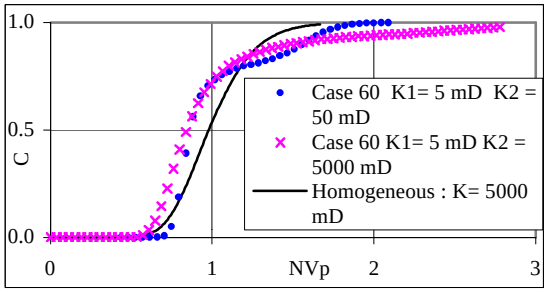

Figure 14 – Case 60, phi2=20%. v= 10^{-6} m/s.
Influence of permeability contrast.

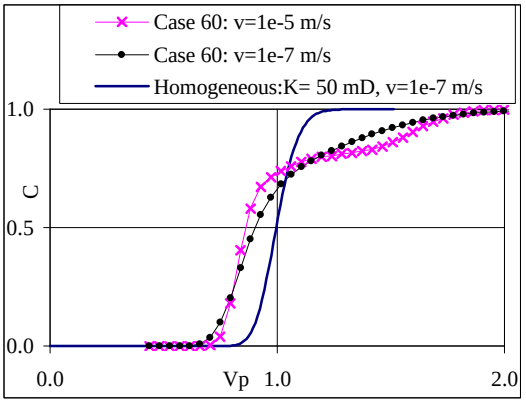

Figure 15 – Case 60, phi2= 20%, K1 = 5 mD, K2 = 50 mD. Influence of v.

From all the direct simulations that have been performed, we can propose the following conclusions :

- Miscible displacements are not sensitive enough to cross section heterogeneity.
- Heterogeneity along the core axis can be easily detected.
- High velocity heightens the differences between regions, so it allows us a better identification of the heterogeneity. This is in agreement with previous works. The various methods developed to extract meaningful information on heterogeneity from miscible displacement curves [Correa & al., 1990, Magnico & al., 1993] suggest that tracer experiments should be carried out at relatively low mass transfer and therefore at high flow rates, in order to distinguish heterogeneous phases.
- the three important parameters -velocity, volume proportion and permeability contrast- have a significant influence on some characteristic parts of the elution curves.

Characterization of heterogeneity from experiments of miscible displacement

The objective of this part of the work is to provide a quantitative characterization of longitudinal heterogeneity from experimental miscible curves. This approach has been carried on a large number of core samples. Only six cases are presented in this work. The following table presents the main characteristics of these samples and the measurements program that has been performed. The table specifies which conclusion about heterogeneity can be drawn from the measurement.

	D1	**D2**	**D3**	**N1**	**A10**	**A2**	**A6**
	Sandstone unconsolidated	Sandstone unconsolidated	Sandstone unconsolidated	Shaly-sandstone	Synthetic	Vuggular dolomite	Vuggular dolomite
K (mD)	3000	8330	6500	193	4300	8.5	29
CT	No evidence of heterogeneity	2 regions	No evidence of heterogeneity	2 regions	N.A	Vugs	Vugs
Probe permeameter	N.A	N.A	N.A	2 regions	Homogeneous	Vugs	Vugs
Miscible	Homogeneous response	Heterogeneous response	Heterogeneous response	Heterogeneous response	Homogeneous	Heterogeneous response	Heterogeneous response

1- Experimental work

The numerical study exposed above shows that high velocity is appropriate to detect lengthwise heterogeneity. The first step is to determine the flow rate to perform the miscible displacement. We used a pore Peclet number, Pep, defined by [Bear, 1972] : $Pep = \frac{u * d_p}{D_d}$, and chose Pep >> 1 to be in a regime of

negligible diffusion. The Kozeny-Carman relation was used to determine a pore characteristic length, d_p, such as : $k = \frac{\varepsilon^3 d_p^2}{(1-\varepsilon)^2 * 180}$

and the minimum flow rate needed for the experiments, Q, was given by : $Q = \varepsilon * S * \frac{D_d * Pep}{d_p}$

Above this indication of a minimum flow rate, the main limitations in the choice of the flow rate sometimes came from the equipment (pump). The other interest in performing miscible experiments at the same order of Peclet, was that it allowed for meaningful comparison between the different samples.

- Experiments on samples D1, D2, D3, N1

All the miscible experiments (figure 16) were carried out at high velocity.

Sample D1 is homogeneous one : its elution curve passes through the C=0.5,Vp=1 point, it is nearly symmetrical around this point and the effluent curve is straight. The miscible response of sample D2 has an early breakthrough, a curved front and a delay before reaching the final concentration (about 2 Vp).

The breakthrough of the curve of sample D3 at 0.7 PV followed by a sharp tail may be relevant of a majoritary high permeable region. The curve of sample N1 presents two steps : a quick breakthrough at 0.5 Vp and a second rapid increase at 1.7 Vp. According to the numerical experiments presented previously, we believe that this is typical of a sample with longitudinal heterogeneity and with moderate permeability contrast.

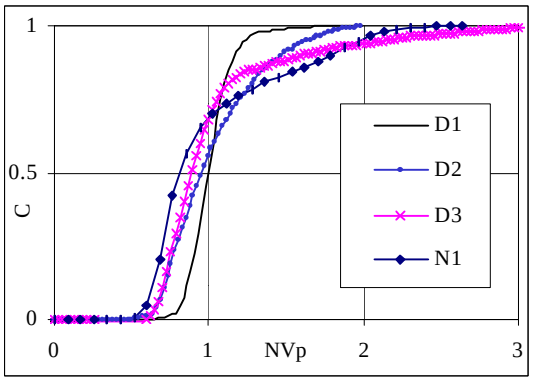

Figure 16 – Experimental curves of miscible displacement : samples D1, D2, D3, N1.

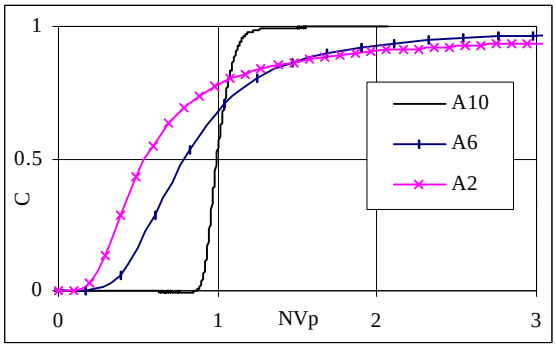

Figure 18 – Experimental miscible curves of vuggy samples A6 and A2, the sample A10 at low velocity.

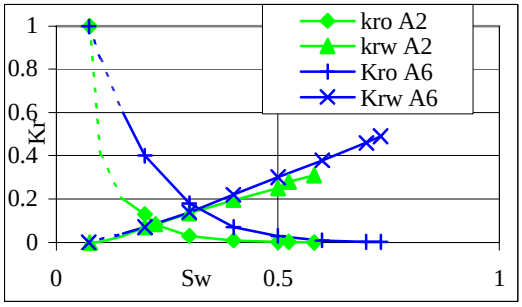

Figure 17 – Relative permeability curves of the vuggy samples A6 and A2 in unsteady-state.

- Experiments on vuggular samples : A2 and A6

Figure 18 presents miscible curves of the 2 vuggy samples with the reference of the homogeneous synthetic sample A10 at mean velocity (Pep<0.1). The miscible response of the sample A2 presents a faster breakthrough (before 0.1 Vp) and a longer tail than sample A6. For sample A2, the very early breakthrough

followed an extremely long tail seems to indicate the existence of a an along-axis, sample spanning very high permeable streak in a tight matrix (see Case 25 of figure 11). Miscible experiments were carried out at higher velocity (Pep >1) : heterogeneity features –breakthrough and tail– of both samples are more pronounced at high velocity. Figure 17 displays the water/oil relative permeability curves of samples A2 and A6 obtained by unsteady-state coreflood experiments. Both samples present early water breakthrough and water saturations start at anomalous low values. Sample A2 presents an oil relative permeability abruptly decreasing. On the contrary, the relative curves of sample A6 do not present any anomaly. Miscible displacements and unsteady-state two-phase experiments are in total agreement : sample A6 appears to be more homogeneous than sample A2.

2- Quantitative analysis of the experimental miscible responses

- Methodology for homogeneous cores

For the homogeneous cores, the interpretation of the miscible curve is made with the 1D homogeneous analytical solution of the convection-dispersion equation (1). It allows to compute the pore velocity and the coefficient of hydrodynamic dispersion. Under the assumption of a negligible molecular diffusion, we compute the longitudinal dispersivity from the coefficient of hydrodynamic dispersion and the seepage velocity, which must be equal to the experimental one.

- Methodology for heterogeneous cores

Some of the miscible experiments presented above display strong anomaly which may be relevant of longitudinal heterogeneity. The objective of this part is to expose the quantification of these heterogeneities. As previously explained, we do not seek for the real heterogeneity but instead the main characteristics such as the volume proportion of high and low permeable regions and the permeability contrast between the heterogeneous zones. The core sample is simplified in a two region model : high and low permeable regions. To identify heterogeneity, we matched a 2D heterogeneous simulated configuration with the experimental miscible curve. The simulation parameters provide the quantitative analysis of the heterogeneous core samples in terms of permeability contrast and volume fraction of each region.

To guide us in matching the experimental miscible curve, we also used qualitative information about the spatial organization of the heterogeneity, from CT scan data and local probe permeameter measurements. In the first part of this work, we have shown that simulated miscible responses have particular form according to the heterogeneity type. These type curves are very helpful to diagnose the plausible heterogeneity configurations. In the input model data, the velocity is the experimental seepage velocity and, when possible, the dispersivities are computed from homogeneous cores representative of the same facies. Simulated permeability and porosity are consistent with the overall ones.

Matching a multi-parameter model to data always raises the question of whether the best fit is unique. In our case, non-uniqueness has a physical basis. By definition, an effluent concentration curve is a large-scale response of the sample so that many local-scale heterogeneities can lead to it. Previous studies [Correa & al., 1990, Magnico & al., 1993] and our numerical work show that heterogeneous zones are more differentiated at high velocities. This may suggest that the heterogeneity configuration determined by fitting a miscible curve performed at high flow rate is more reliable. So, to reduce the doubt about the uniqueness of the solution, whenever it is possible, we match the multi-parameter model to experimental data performed at high velocity and we consider CT scan and local permeability surface maps to validate heterogeneity geometry. The best validation for plausible heterogeneous configuration is when it directly matches the experimental miscible curves at two different flow rates.

- Quantitative interpretation of heterogeneity of samples D1, D2, D3 and N1.

Sample D1 presents homogeneous experimental miscible response, so we interpreted it with the 1D analytical solution (figure 19). We obtained a dispersivity of 0.2 cm and a seepage velocity of $1.4.10^{-5}$ m/s for a permeability of 3 D.

The experimental and simulated curves of sample D2 are represented in figure 20. The heterogeneity geometrical configuration (figure22) is based on the CT scan cross-section images (figure 21). Sample D2 resembles sample D1 in permeability and textural properties, so the dispersivity is assumed to be the same.

Heterogeneity configuration is found with a tenfold permeability contrast and a volume proportion of the very permeable region of 45%.

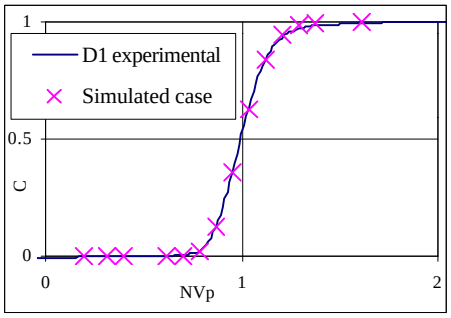

Figure 19 – Homogeneous sampleD1 : Experimental and simulated curves. $v=1.4.10^{-5}$ m/s, $D=8.10^{-8}$ m^2/s.

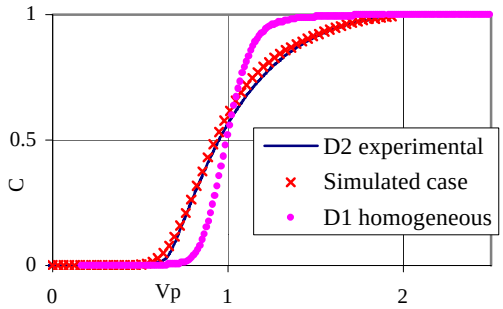

Figure 20 – Sample D2 :Experimental and simulated curves. $v=4.10^{-8}$ m/s, K2/K1= 10, phi2= 45%.

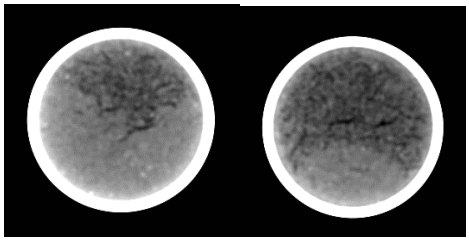

Figure 21 – Sample D2 : cross-section CT scan image at x=10 cm and x=15 cm at a 30 cm total length.

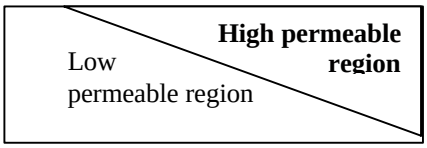

Figure22 – Geometry of sample D2.

Sample D3 (figure 23), close to sample D1 in permeability and textural properties, has its dispersivity deduced from sample D1. The heterogeneity geometry and the simulation's parameters which matched the experimental curve are shown in figures 24 and 23. Even if the tenfold permeability contrast is the same as sample D2, the miscible response of sample D3 is totally different because of a majority proportion of high permeable region (60%).

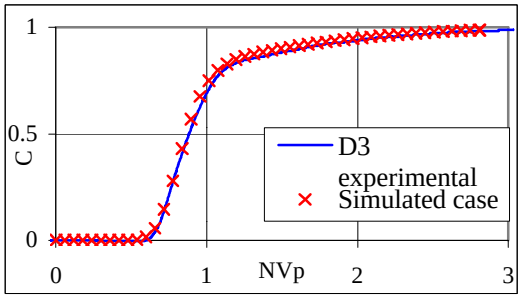

Figure 23 – Sample D3 :Experimental and simulated curves. v=10^{-7} m/s, K2/K1= 10, phi2 = 60%.

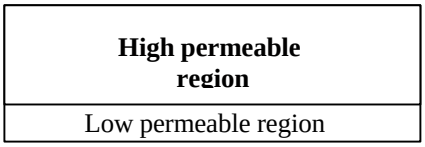

Figure 24 – Geometry of sample D3.

For sample N1, the heterogeneity configuration is illustrated on figure 27. This heterogeneity configuration is a perfect match of the experimental and simulated curves either at mean (figure 25) or high velocity (figure 26). The permeability contrast between the two regions is about 10, the high permeable zone has a volume of 22%. The CT scan data (figure 28) totally agree with the geometry of heterogeneity.

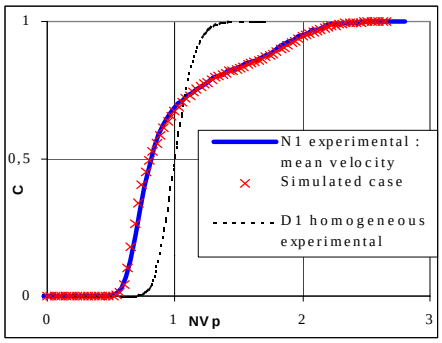

Figure 25 –Sample N1 : Experimental and simulated curves at a mean velocity. v=3.10^{-7} m/s, K2/K1= 10, phi2 = 20%.

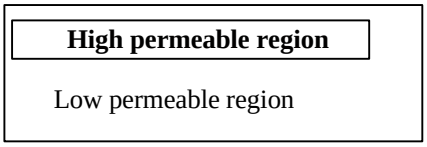

Figure27 – Geometry of sample N1.

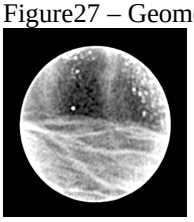

Figure 28 – Sample N1 : cross-section CT scan image at x=7 cm for a 16 cm total length.

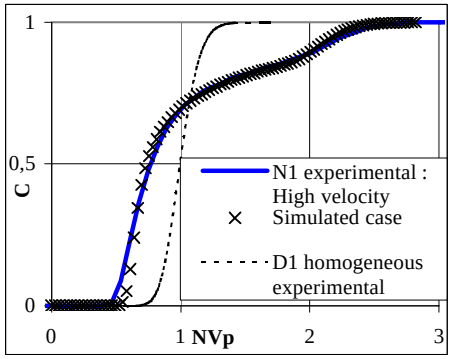

Figure 26 – Sample N1 :Experimental and simulated curves at a high velocity. v=7.10^{-7} m/s, K2/K1= 10, phi2 = 20%.

- Quantitative interpretation of heterogeneity of the vuggy samples A6 and A2.

CT scan images and local permeability surface maps show no difference between the core samples A2 and A6 [Dauba & al., SCA9828, 1998] : they both present a lot of mean size vugs without any particular spatial distribution. However, miscible experiment in agreement to two-phase displacements reveals that sample A2 is more heterogeneous than sample A6 (figures 17 and 18).

Sample A2 has the same large-scale behavior as an along-axis, sample spanning very highly permeable streak in a tight matrix (figure 30). The very high permeable region represents only 3% of the volume but the permeability contrast is extremely high, about 1000. This heterogeneous 2D configuration matches the experimental miscible responses at both low (figure 29) and high velocities. We can deduce that this preferential path is made of some vugs especially well connected with each other by micro-fissures.
For the vuggy sample A6, the heterogeneity case which corresponds to the experimental miscible curves (figure 31) is described on figure 32 : an along-axis, sample spanning permeable region is embodied in a low permeable matrix and it is divided into four thin preferential paths in order to increase the mass transfer. The permeability contrast is of 100, the high permeability region represents 16% of the whole. The 2D heterogeneous case matched miscible experiments at both mean and high velocity (figure 31). This suggests that vugs of sample A6 are not very connected with each other and spread into the matrix. This leads to an effluent curve trending to “homogeneous” response because of high mass exchange and low contrast between the matrix and the preferential paths.
This illustrates the inefficiency of CT scan data to characterize the dynamic heterogeneity of vuggy core samples.

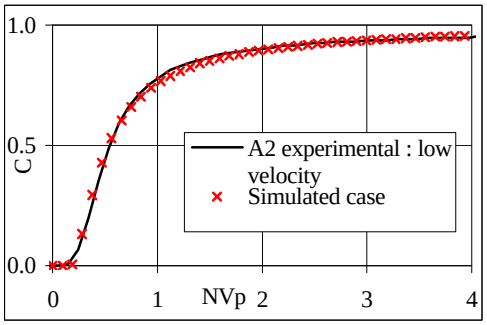

Figure 29 – Sample A2 :Experimental and simulated curves at a low velocity. $v=6.10^{-7}$ m/s,K2/K1= 1000, phi2 = 3%.

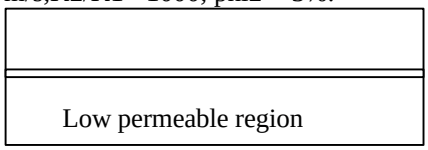

Figure 30 – Geometry of sample A2.

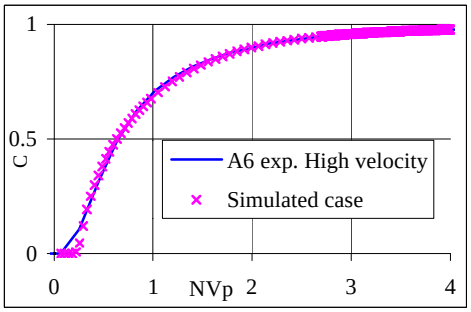

Figure 31 – Sample A6 :Experimental and simulated curves at high velocity. $v=1.5.10^{-6}$ m/s, K2/K1=100, phi2 = 16%.

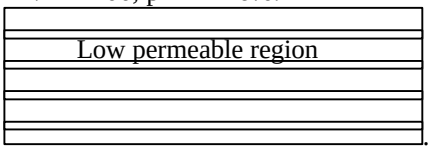

Figure 32 – Geometry of sample A6.

Considering the following approach, we managed to interpret experimental miscible curves with a 2D heterogeneous model :

1. A lot of type curves have been computed by direct simulation. They illustrate the impact of the heterogeneity geometry, permeability contrast, the volume proportion and the velocity.
2. These type curves were very helpful to diagnose the plausible heterogeneity configurations from experimental tracer concentration curves.
3. The most likely configurations were selected using CT scan information or probe permeameter data.
4. The core was simplified to a two regions model : a high permeable region and a low permeable one.
5. History matching of experimental effluent curve was carried out to get permeability contrast and volume fraction of each region.

6. This approach results in a simplified representation of an heterogeneous core, but totally consistent with the CT images, probe permeameter data if available, overall porosity and permeability and the sample response to miscible tracer experiments.

Conclusion

The following conclusions were drawn :

1) The tracer experiment is an excellent indicator of the lengthwise heterogeneity. On the contrary, it is not very sensitive to cross-section heterogeneity.

2) Miscible displacement is a very simple means of dynamic identification of the most heterogeneous samples. Performing miscible displacement can avoid long and expensive waterflooding tests, inevitably doomed to failure because of strong longitudinal heterogeneity.

3) With indications from type curves and from other sources (CT scan data, probe permeameter measurements,…etc), we interpret experimental miscible responses and model heterogeneous core samples in a configuration with two mobile regions. This method allows us to compute the permeability contrast and the volume proportion of each region. Thus, for heterogeneous core samples, it will now be possible to interpret the relative permeability curves with a 2D heterogeneous model.

Acknowledgments

We are especially grateful to Jerome David, Pascal Maurin, Didier Lasseux and Catherine Prinet for their help. We would also like to thank Elf Exploration Production and Total for their financial support and for their permission to publish this work.

Nomenclature

C	tracer concentration, ML^{-3}
D	coefficient of hydrodynamic dispersion, L^2T^{-1}, $D = \alpha_L * v + D_d$
D_d	coefficient of molecular diffusion, L^2T^{-1}
k	permeability, L^2
kr	relative permeability
K1	permeability of the low permeable region.
K2	permeability of the high permeable region.
L	length of the core, L
Pe	Peclet number $Pe = v*L/D'$
Pep	pore Peclet number $Pep = u*d_p/D_d$
phi2	volume proportion of high permeable region.
Vp	pore volume (or NVp)
Q	flow rate
S	section of the core, L^2.
t	time, T
u	pore velocity, LT^{-1}
v	seepage velocity, LT^{-1} $v = u*\varepsilon$
x	longitudinal distance, L

Greek letters

α_L	longitudinal dispersivity of an isotropic medium, L.
ε	porosity, dimensionless
τ	dimensionless time $\tau = v*t/(\varepsilon*L)$

References

Baker L.E., “Effects of dispersion and dead end pore volume in miscible flooding”, *Soc. Pet. Eng. J. Tran.* AIME **263**, 219 (1975).

Bear J., “Dynamics of Fluids in Porous Media”, (Elsevier, New York, 1972), Chap. 10.

Coats K.H., Smith B.D, “Dead-end pore volume and dispersion in porous media”, *Soc. Pet. Eng. J.* Trans. AIME **231**, 73 (1964).

Correa A.C., Pande K.K., Ramey Jr. H.J., Brigham W.E., “Computation and interpretation of miscible displacement performance in heterogeneous porous media”, *SPEFE*, Feb. 1990, 69-78.

Dauba C., Hamon G., Quintard M., Lasseux D., “Stochastic description of experimental 3D permeability fields in vuggy reservoir cores”, *SCA 9828*, 1998 Symp. Soc. Core Analysts, The Hague, Netherlands, Sept. 13-16, 1998.

Gerke H.H., van Genuchten M.T., “A dual-porosity model for simulating the preferential movement of water and solutes in structured porous media”, *Water Resour. Res.*, (1993), vol. **29**, No 2, 305-319.

Magnico P., Leroy C., Bouchaud J.P., Gauthier C., Hulin J.P., “Tracer dispersion in porous media with a double porosity”, *Phys. Fluids*, A **5** (1), Jan. 1993.
Mennela A., Bryant S.L., Lockhart T.P., “Propagation of tracers through cores with mass transfer into an immobile fluid phase”, *SPE 37248*, 1997 SPE Int. Symp. Oilfield Chemistry, Houston, USA, Feb. 18-21, 1997.
Quintard M., Ahmadi A., Whitaker S.,“Transport in chemically and mechanically heterogeneous porous media. Part V : Two-equation model for solute transport with adsorption”, *Water Resour. Res.*, (1998), vol. **22**, 59-86.